

DOI:10.1002/ejic.201300254

Mechanistic Studies on the Reaction of Nitrocobalamin with Glutathione: Kinetic Evidence for Formation of an Aquacobalamin Intermediate

David T. Walker,^{[a]‡} Rohan S. Dassanayake,^{[a]‡}
Kamille A. Garcia,^[a] Riya Mukherjee,^[a] and Nicola E. Brasch*^[a,b]

Keywords: Vitamin B₁₂ / Cob(III)alamin / Bioinorganic chemistry / Kinetics / Reaction mechanisms

The essential but also toxic gaseous signaling molecule nitric oxide is scavenged by the reduced vitamin B₁₂ complex cob(II)alamin. The resulting complex, nitrosylcobalamin [NO-Cbl(III)], is rapidly oxidized to nitrocobalamin (NO₂Cbl) in the presence of oxygen; however, it is unlikely that nitrocobalamin is itself stable in biological systems. Kinetic studies on the reaction between NO₂Cbl and the important intracellular antioxidant, glutathione (GSH), are reported. In this study, a reaction pathway is proposed in which

the β-axial ligand of NO₂Cbl is first substituted by water to give aquacobalamin (H₂O Cbl⁺), which then reacts further with GSH to form glutathionylcobalamin (GSCbl). Independent measurements of the four associated rate constants k_1 , k_{-1} , k_2 , and k_{-2} support the proposed mechanism. These findings provide insight into the fundamental mechanism of ligand substitution reactions of cob(III)alamins with inorganic ligands at the β-axial site.

Introduction

Two essential enzymes in mammals, L-methylmalonyl-CoA mutase and methionine synthase, and numerous bacterial enzymes require the vitamin B₁₂ derivatives (= cobalamins, Cbls) adenosylcobalamin (AdoCbl) and methylcobalamin (MeCbl) as cofactors, Figure 1.^[1] MeCbl-dependent methionine synthase transfers a methyl group from methyltetrahydrofolate to homocysteine to generate tetrahydrofolate and methionine, whereas AdoCbl-dependent L-methylmalonyl-CoA mutase catalyzes the isomerization of L-methylmalonyl-CoA to succinyl-CoA.^[1] Cobalamins may also have additional roles in biological systems, including regulating the immune response and protecting against intracellular oxidative stress.^[2]

The signaling molecule nitric oxide (·NO) plays a key role in the immune response, vasodilation, and neurotransmission.^[3] However, high levels of NO can be deleterious and can result in sepsis and septic shock,^[4] which leads to organ failure and even death. Importantly, administering cobalamins suppresses ·NO-induced relaxation of smooth muscle,^[5] ·NO-induced vasodilation^[6] and ·NO-mediated inhibi-

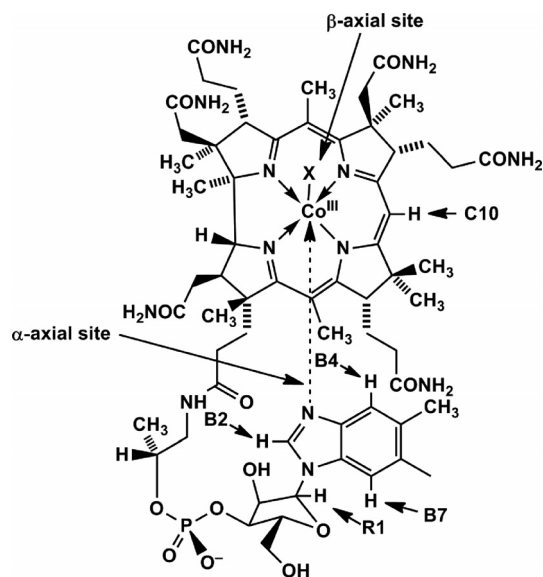


Figure 1. Structure of cobalamins showing the two axial sites (upper = β, lower = α) with respect to the corrin ring.

tion of cell proliferation.^[7] Cobalamins also reverse ·NO-induced neural tube defects.^[8] Both mammalian B₁₂-dependent enzymes are inhibited by ·NO.^[9] With the exception of glutathionylcobalamin (X = glutathione, Figure 1), ·NO does not directly react with cob(III)alamins,^[10] whereas the rate of the reaction between cob(II)alamin and nitric oxide to form nitrosylcobalamin (NOCbl) is almost diffusion controlled and essentially irreversible.^[11] Given

[a] Department of Chemistry and Biochemistry, Kent State University, Kent, OH 44242, USA

[b] School of Biomedical Sciences, Kent State University, Kent, OH 44242, USA
E-mail: nbrasch@kent.edu
Homepage: www.brasch-group.com

‡ Equal contributions

Supporting information for this article is available on the WWW under <http://dx.doi.org/10.1002/ejic.201300254>.

that all cob(III)alamins are readily reduced by intracellular reductases,^[12] it is likely that cob(II)alamin reacts with NO in biological systems, to form NOCbl.

In discussions of the biological relevance of NOCbl formation, we have observed that authors neglect to mention that NOCbl itself is not a stable entity.^[5a,6–8,9c–9e] However, in the presence of even minute amounts of air, orange NOCbl rapidly oxidizes to form red nitrocobalamin, NO₂Cbl.^[13] Indeed, we have used this property of NOCbl in our laboratory numerous times to check the condition of valves and taps used in strictly anaerobic experimental setups. The intracellular fate of NO₂Cbl is unclear. Possibilities include reduction of NO₂Cbl by intracellular reductases, and/or the reaction of NO₂Cbl with the strong nucleophile and reductant glutathione (GSH), which is present in mM concentrations in cells.^[14] In this work, we report kinetic studies on the reaction of NO₂Cbl with glutathione. Interestingly, our kinetic data show that GSH does not directly react with NO₂Cbl, but instead reacts with aquacobalamin, which is always present in equilibrium, albeit typically in small amounts, in cobalamins with inorganic ligands at the β-axial cobalamin site (Figure 1).

Results and Discussion

Kinetic data were collected for the reaction of NO₂Cbl with glutathione (GSH). Experiments were initiated by adding a small aliquot of concentrated aqueous NO₂Cbl solution (final concentration 5.0×10^{-5} M) to a buffered GSH solution (3.00 mL) at a specific pH condition [$I = 1.0$ M (NaCF₃SO₃)]. Control experiments established that rate constants were identical within experimental error in the absence and presence of air; hence, all experiments were carried out under aerobic conditions. Importantly, the dissolving of NO₂Cbl in water rather than in buffer minimized the decomposition of NO₂Cbl to aquacobalamin (H₂OCbl⁺) prior to the addition of an aliquot of this solution into a buffered GSH solution.

Figure 2(a) shows UV/Vis spectral changes observed upon the addition of NO₂Cbl to a buffered GSH solution (5.00×10^{-2} M) at pH 4.00. NO₂Cbl ($\lambda_{\text{max}} = 354, 413, \text{ and } 532$ nm) is converted to GSCbl ($\lambda_{\text{max}} = 333, 372, 428, \text{ and } 534$ nm^[15]) with isosbestic points at 336, 367, 452, and 543 nm, which indicates that a single reaction occurs. The corresponding plot at 354 nm vs. time is given in Figure 2(b). The data fit well to the first-order rate equation, which gives an observed rate constant, $k_{\text{obs}} = (1.15 \pm 0.07) \times 10^{-2} \text{ s}^{-1}$.

Kinetic data were collected at pH 4.00 and 7.00, in order to determine whether the rate of the reaction is pH dependent. Plots of k_{obs} vs. total GSH concentration are shown in Figure 3(a) and (b). These plots indicate that the observed rate constant reaches a limiting value at high GSH concentrations and that there is no pH dependence in this pH region. There are two plausible mechanisms by which NO₂Cbl reacts with GSH to give a plot exhibiting curvature to reach a limiting value of k_{obs} at high GSH concentrations

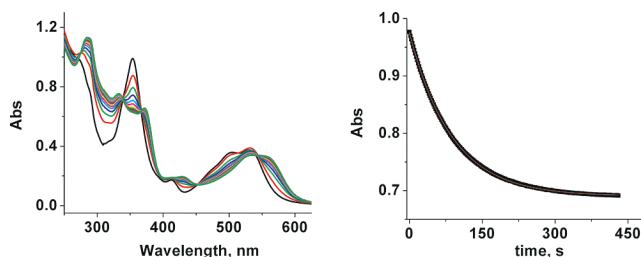


Figure 2. (a) UV/Vis spectra for the reaction of GSH (5.00×10^{-2} M) with NO₂Cbl (5.0×10^{-5} M) at pH 4.00 (25.0 °C, 0.020 M NaOAc, $I = 1.0$ M, NaCF₃SO₃). Selected spectra for the reaction are shown every 1.00 min. (b) Plot of absorbance at 354 nm vs. time for the experiment shown in (a). Data were fitted to a first-order rate equation, which gives $k_{\text{obs}} = (1.15 \pm 0.07) \times 10^{-2} \text{ s}^{-1}$.

(saturation kinetics). The first involves rapid equilibration to form a NO₂Cbl·GSH association complex prior to rate-determining substitution of the β-axial NO₂⁻ ligand of NO₂Cbl by GSH to give GSCbl. The other alternative is a two-step process, in which H₂OCbl⁺, which is in equilibrium with NO₂Cbl, reacts with GSH (Scheme 1). Given that all Cbls with β-axial inorganic ligands exist in equilibrium with H₂OCbl⁺ and that Cbls undergo β-axial ligand exchange through a dissociative interchange mechanism,^[16] the latter possibility is more likely to occur. Kinetic studies on the reaction between H₂OCbl⁺/HOCbl and GSH have been reported^[17] and show that H₂OCbl⁺ reacts rapidly with GSH to form GSCbl under the conditions of our study.

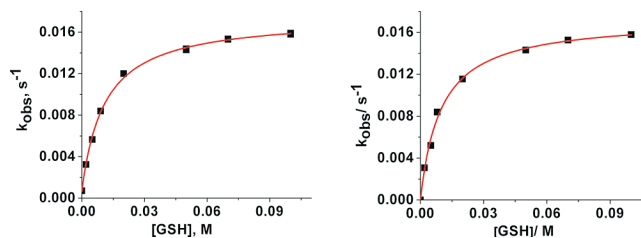


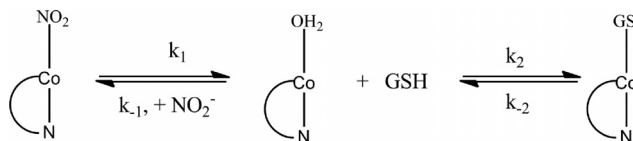
Figure 3. Plots of k_{obs} vs. [GSH] at pH (a) 4.00 and (b) 7.00 for the reaction between NO₂Cbl (5.00×10^{-5} M) and glutathione [25.0 °C, (a) 0.020 M NaOAc or (b) 0.020 M KH₂PO₄, $I = 1.0$ M (NaCF₃SO₃)]. Data in (a) were fitted to Equation (2) in the text fixing $k_{-2} = 7.4 \times 10^{-4} \text{ s}^{-1}$, which gives $k_1 = (1.75 \pm 0.02) \times 10^{-2} \text{ s}^{-1}$ and $K = 94.5 \pm 3.7 \text{ M}^{-1}$ at pH 4.00. Data in (b) were fitted to Equation (2) fixing $k_{-2} = 0 \text{ s}^{-1}$, which gives $k_1 = (1.73 \pm 0.05) \times 10^{-2} \text{ s}^{-1}$ and $K = 102.1 \pm 9.7 \text{ M}^{-1}$ at pH 7.00.

The rate expression corresponding to the reaction pathway shown in Scheme 1 is shown in Equation (1).^[18]

$$k_{\text{obs}} = \{k_1 k_2 [\text{GSH}] / (k_{-1} [\text{NO}_2^-] + k_{-2})\} / \{1 + k_2 [\text{GSH}] / (k_{-1} [\text{NO}_2^-])\} \quad (1)$$

$$= (k_1 K [\text{GSH}] + k_{-2}) / (1 + K [\text{GSH}]) \quad (2)$$

where $K = k_2 / (k_{-1} [\text{NO}_2^-])$. The rate constant, k_{-2} , for decomposition of GSCbl to H₂OCbl⁺ and GSH was independently determined at pH 4.00 and found to be $(7.4 \pm 0.5) \times 10^{-4} \text{ s}^{-1}$ (Figure S1, Supporting Information).



Scheme 1. Proposed reaction pathway for the reaction of NO_2Cbl with GSH. Note that in aqueous solution H_2OCbl^+ exists in equilibrium with HOCbl [$\text{p}K_{\text{a}}(\text{H}_2\text{OCbl}^+) = 7.8^{[17]}$]; however, at the pH conditions of our kinetic experiments, HOCbl formation is unimportant, since the values of the rate constants k_{-1} and k_2 are the same at pH 4.00 and 7.00.

Previous studies have shown that the observed equilibrium constant for formation of GSCbl , $K_{\text{obs}}(\text{GSCbl}) = k_2/k_{-2}$, increases by approximately one order of magnitude for each unit change in pH.^[17] Since k_2 is pH independent,^[17] k_{-2} is therefore negligible at pH 7.00. Data in Figure 3(a) were fitted to Equation (2) by fixing $k_{-2} = 7.4 \times 10^{-4} \text{ s}^{-1}$, which gives $k_1 = (1.75 \pm 0.02) \times 10^{-2} \text{ s}^{-1}$ and $K = 94.5 \pm 3.7 \text{ M}^{-1}$. Data in Figure 3(b) were fitted to the same equation by fixing $k_{-2} = 0 \text{ s}^{-1}$, which gives $k_1 = (1.73 \pm 0.05) \times 10^{-2} \text{ s}^{-1}$ and $K = 102.1 \pm 9.7 \text{ M}^{-1}$. K is therefore also pH independent in the pH 4–7 region, within experimental error.

Importantly, if our model is correct, then $K = k_2/(k_{-1}[\text{NO}_2^-])$. Note, however, that the free nitrite concentration is not strictly constant during the reaction, but will vary from 0 to a maximum value of $5.0 \times 10^{-5} \text{ M}$ as the reaction proceeds, as NO_2Cbl ($5.0 \times 10^{-5} \text{ M}$) reacts with GSH to give GSCbl plus NO_2^- . Hence, K is not strictly constant during the reaction, as reflected in the error associated with K . In order to provide support for our model, new data was therefore collected at pH 7.00 under the same conditions as the experiments summarized in Figure 3(b), except that $5.00 \times 10^{-4} \text{ M}$ NaNO_2 was added to each solution, so the nitrite concentration is constant (pseudo-first order conditions) during the reaction. These data are shown in Figure 4. Fitting of this data to Equation (2) by fixing $k_{-2} = 0 \text{ s}^{-1}$ gave $k_1 = (1.60 \pm 0.05) \times 10^{-2} \text{ s}^{-1}$ and $K = 16.2 \pm 0.2 \text{ M}^{-1}$. The data now fit considerably better to Equation (2) as expected (the error in K is now one order of magnitude smaller), since the nitrite concentration remains constant during the reaction.

The rate constant k_2 for the reaction of H_2OCbl^+ with GSH was also independently determined at pH 4.00 and found to be $12.00 \pm 0.25 \text{ M}^{-1} \text{ s}^{-1}$ [25.0 °C, 0.020 M NaCH_3COO , $I = 1.00 \text{ M}$ (NaCF_3SO_3)] (Figure S2, Supporting Information). This value is in good agreement with a value reported by us under slightly different conditions [$k_2 = 18.5 \text{ M}^{-1} \text{ s}^{-1}$ at pH 4.50, 25.0 °C, 0.10 M NaOAc , $I = 0.50 \text{ M}$ (KNO_3)^[17]], and is pH independent in the pH 4–7 range.^[17] The rate constant k_{-1} for the reaction between H_2OCbl^+ and NO_2^- was independently determined to be $(1.25 \pm 0.02) \times 10^3$ and $(1.20 \pm 0.02) \times 10^3 \text{ M}^{-1} \text{ s}^{-1}$ at pH 4.00 and 7.00, respectively (Figures S3 and S4, Supporting Information). Hence, k_{-1} is also independent of the pH (pH 4–7), as expected, as the ionization of the reactants is essentially unchanged [$\text{p}K_{\text{a}}(\text{HNO}_2) \approx 3.2$; $\text{p}K_{\text{a}}(\text{H}_2\text{OCbl}^+) = 7.8^{[17]}$] in this pH region. The value of k_{-1} agrees well with a value

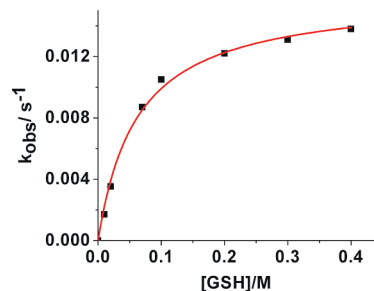


Figure 4. Plot of k_{obs} vs. $[\text{GSH}]$ for the reaction between NO_2Cbl ($5.0 \times 10^{-5} \text{ M}$) and GSH in the presence of $5.00 \times 10^{-4} \text{ M}$ NaNO_2 at pH 7.00 (25.0 °C, 0.020 M KH_2PO_4 , $5.00 \times 10^{-4} \text{ M}$ NaNO_2 , $I = 1.0 \text{ M}$, NaCF_3SO_3). Data were fitted to Equation (2) in the text by fixing $k_{-2} = 0$, which gives $k_1 = (1.60 \pm 0.05) \times 10^{-2} \text{ s}^{-1}$ and $K = 16.2 \pm 0.2 \text{ M}^{-1}$.

reported by others [$k_{-1} = 99.8 \times 10^2 \text{ M}^{-1} \text{ s}^{-1}$ at 25 °C, $I = 2.2 \text{ M}$ (NaNO_3)].^[19] By using $k_2 = 12.00 \text{ M}^{-1} \text{ s}^{-1}$, $k_{-1} = 1.23 \times 10^3 \text{ M}^{-1} \text{ s}^{-1}$, and $[\text{NO}_2^-] = 5.00 \times 10^{-4} \text{ M}$, a value of $K \approx 20 \text{ M}^{-1}$ is obtained, which is in very good agreement with the experimental value of K obtained from the best fit of the data ($16.2 \pm 0.2 \text{ M}^{-1}$) and provides strong support for the reaction pathway proposed in Scheme 1.

Finally, the rate constant k_1 for decomposition of NO_2Cbl to H_2OCbl^+ was also independently determined by obtaining kinetic data for the decomposition of NO_2Cbl to H_2OCbl^+ upon dissolving NO_2Cbl in buffer. Figure S5 (Supporting Information) shows the absorbance change ($\Delta\text{Abs} = 0.013$ at 350 nm) that occurs at pH 4.00. Only a small fraction of NO_2Cbl is converted to H_2OCbl^+ ; however, the absorbance change is sufficient to allow calculation of k_1 . The results at different pH conditions are summarized in Table S1 and give a mean value for k_1 of $(1.48 \pm 0.22) \times 10^{-2} \text{ M}^{-1} \text{ s}^{-1}$ (pH 3.5–6.0; k_1 is pH independent). The observed rate constant for the partial decomposition of NO_2Cbl to give H_2OCbl^+ is actually $(k_1 + k_{-1}[\text{NO}_2^-])$ for the pseudo-first-order reversible process. A separate experiment showed that an absorbance difference of 0.232 is observed upon completely converting H_2OCbl^+ to NO_2Cbl upon the addition of a slight excess of NO_2^- ($[\text{Cbl}]_{\text{T}} = 5.0 \times 10^{-5} \text{ M}$). Hence, an absorbance change of 0.013 corresponds to formation of 5.6% H_2OCbl^+ ($2.8 \times 10^{-6} \text{ M}$ H_2OCbl^+ and $2.8 \times 10^{-6} \text{ M}$ NO_2^-) upon dissolving NO_2Cbl in H_2OCbl^+ ; that is, the maximum NO_2^- is $2.8 \times 10^{-6} \text{ M}$. For $k_1 = 1.48 \times 10^{-2} \text{ M}^{-1} \text{ s}^{-1}$, $k_{-1} = (1.25 \pm 0.02) \times 10^3$ and $[\text{NO}_2^-] = 2.8 \times 10^{-6} \text{ M}$ k_1 is about 5 times larger than $k_{-1}[\text{NO}_2^-]$, which validates the assumption that $k_{\text{obs}} \approx k_1$ upon dissolving NO_2Cbl in H_2OCbl^+ . By using our values of k_1 and k_{-1} , the equilibrium constant for formation of NO_2Cbl , $K(\text{NO}_2\text{Cbl}) = k_{-1}/k_1$, is $8.5 \times 10^4 \text{ M}^{-1}$, which is in reasonable agreement with a value reported by others under different ionic strength conditions [$K(\text{NO}_2\text{Cbl}) = 2.2 \times 10^5 \text{ M}^{-1}$, 25 °C, $I = 2.2 \text{ M}$]^[20].

Conclusions

Kinetic studies on the reaction between NO_2Cbl and GSH show that the rate of the reaction is pH independent

in the pH 4–7 region. By independently determining values of k_1 , k_{-1} , k_2 , and k_{-2} , we have shown that the data fits a model involving an H_2OCbl^+ intermediate, which then rapidly reacts with GSH to form GSCbl (Scheme 1). To our knowledge, this is the first time that the reaction pathway of β -axial inorganic ligand exchange for cob(III)alamins via an H_2OCbl^+ intermediate has been unequivocally demonstrated. This may have important consequences for free and potentially for even protein-bound cob(III)alamins incorporating inorganic ligands (X-ray structures of cobalamins bound to B_{12} transport proteins show that the β -axial site can be readily accessed by solvent and small molecules^[21]); that is, the amount of each of these species may reflect the concentrations and binding constants to aquacobalamin of the various inorganic ligands present. As such, GSCbl would be expected to be the major intracellular non-alkyl-cob(III)alamin, given that intracellular GSH concentrations are in the mM region,^[14] and only CN^- binds more strongly than GSH to H_2OCbl^+ ($K_{\text{CN/Cbl}} \approx 10^{14} \text{ M}^{-1}$ ^[22]). Finally, at 0.5 mM GSH, the rate constant for the reaction between NO_2Cbl and GSH is $\approx 8 \times 10^{-3} \text{ s}^{-1}$ at pH 7.0 (25 °C), which corresponds to a half-life of about 1.4 min. Hence, formation of GSCbl is one possible reaction pathway by which NO_2Cbl decomposes in biological systems.

Experimental Section

General: Hydroxycobalamin hydrochloride ($\text{HOCbl}\cdot\text{HCl}$, 98% stated purity by manufacturer) was purchased from Fluka. Glutathione (98%), acetic acid (sodium salt, $\geq 99\%$), sodium nitrite (97%), and $\text{CF}_3\text{SO}_3\text{H}$ (99%) were obtained from Acros Organics. TES buffer (98%) was purchased from MP Biomedicals Inc. Potassium dihydrogen phosphate was purchased from Sigma. NaCF_3SO_3 was prepared by neutralizing a concentrated, aqueous solution of $\text{CF}_3\text{SO}_3\text{H}$ with NaOH, by reducing it to dryness by rotary evaporation, and by drying it overnight in a vacuum oven at 70.0 °C. Nitrocobalamin was synthesized and characterized according to a published procedure.^[15] The purity was $\geq 95\%$, as determined by ^1H NMR spectroscopy.

UV/Vis spectra and kinetic data for slower reactions were recorded on a Cary 5000 spectrophotometer equipped with a thermostatted (25.0 ± 0.1 °C) cell changer operating with WinUV Bio software (version 3.00). Reactant solutions were thermostatted for 15 min prior to measurements. Kinetic data for rapid reactions were obtained at 25.0 ± 0.1 °C by using an Applied Photophysics SX20 stopped-flow spectrophotometer equipped with a photodiode array detector in addition to a single wavelength detector. Data were collected with Pro-Data SX (version 2.1.4) and Pro-Data Viewer (version 4.1.10) software, and a 1.0 cm pathlength cell was utilized. All data were analyzed by using Microcal Origin version 8.0.

pH measurements were carried out by using an Orion model 710A pH meter equipped with a Wilmad 6030–02 pH electrode. The electrode was filled with a 3 M KCl/saturated AgCl solution (pH 7.0) and standardized with standard BDH buffer solutions at pH 6.98, 4.01, and 2.02. Solution pH was adjusted by using 50% v/v aqueous $\text{CF}_3\text{SO}_3\text{H}$ and NaOH ($\approx 5 \text{ M}$).

^1H NMR spectra was recorded on a Bruker Avance 400 MHz spectrometer equipped with 5 mm probe. Solutions for NMR measurements were prepared in D_2O . ^1H NMR spectra were internally referenced to TSP ($\delta = 0$ ppm).

Kinetic Measurements: The rates of the reaction between NO_2Cbl and glutathione (GSH) were determined under pseudo-first-order conditions with excess GSH. Stock solutions of GSH (0.500 M) in the presence or absence of sodium nitrite ($5.00 \times 10^{-4} \text{ M}$) were prepared in the appropriate buffer (0.020 M) at pH 4.00 and 7.00 and diluted as appropriate. A small aliquot of concentrated NO_2Cbl (final concentration $5.0 \times 10^{-5} \text{ M}$) in water was added to initiate the reaction, and the absorbance at 354 nm was recorded as a function of time.

Kinetic data for the reaction between H_2OCbl^+ ($5.0 \times 10^{-5} \text{ M}$) with varying concentrations of NO_2^- were obtained at pH 4.00 and 7.00. Stock solutions of NaNO_2 (0.010 M) were prepared in the appropriate buffer (0.020 M) and diluted as needed. Data were collected at 354 nm. Kinetic data for the reaction of H_2OCbl^+ ($5.0 \times 10^{-5} \text{ M}$) with varying concentrations of glutathione at pH 4.00 were collected at 354 nm in acetate buffer (0.020 M).

The rate of decomposition of NO_2Cbl to H_2OCbl^+ was determined in the pH 3.5–6.0 range by adding solid NO_2Cbl directly to the appropriate buffer solution (0.200 M; the solution was thermostatted at 25.0 °C for 10 min prior to the addition of NaNO_2). The solution was quickly filtered through a micropore filter (0.45 μm), and data collection initiated at 354 nm.

The rate of decomposition of GSCbl to H_2OCbl^+ was determined at pH 4.00. An aliquot of GSCbl ($4.0 \times 10^{-5} \text{ M}$) was added to pH 4.00 acetate buffer (0.020 M; the buffer solution was thermostatted at 25.0 °C for 10 min prior to the addition of GSCbl), and data were collected at 354 nm.

The total ionic strength was maintained at 1.0 M by using NaCF_3SO_3 for all solutions.

Supporting Information (see footnote on the first page of this article): Further kinetic plots, UV/Vis spectra and rate constants are presented.

Acknowledgments

This research was funded by the US National Science Foundation (CHE-084839) and the US National Institute of General Medical Sciences of the National Institutes of Health (1R15GM094707-01A1). The content is solely the responsibility of the authors and does not necessarily represent the official views of the National Institutes of Health. Funding for this work was also provided by the NSF-REU program at KSU [CHE-1004987 (D. W.) and CHE-0649017 (K. G.)].

- [1] a) B. Kräutler, S. Ostermann, *The Porphyrin Handbook* (Eds.: K. M. Kadish, K. M. Smith, R. Guilard), Academic Press, San Diego, **2003**, ch. 68, p. 229; b) R. Banerjee (Ed.), *Chemistry and Biochemistry of B_{12}* , Wiley & Sons, New York, **1999**; c) K. L. Brown, *Chem. Rev.* **2005**, *105*, 2075.
- [2] a) G. Scalabrino, E. Mutti, D. Veber, L. Aloe, M. M. Corsi, S. Galbiati, G. Tredici, *Neurosci. Lett.* **2006**, *396*, 153; b) G. Scalabrino, M. Peracchi, *Trends Mol. Med.* **2006**, *12*, 247; c) D. Veber, E. Mutti, L. Tacchini, E. Gammella, G. Tredici, G. Scalabrino, *J. Neurosci. Res.* **2008**, *86*, 1380–1387; d) R. Mukherjee, N. E. Brasch, *Chem. Eur. J.* **2011**, *17*, 11673; e) C. S. Birch, N. E. Brasch, A. McCaddon, J. H. H. Williams, *Free Radical Biol. Med.* **2009**, *47*, 184; f) E. S. Moreira, N. E. Brasch, J. Yun, *Free Radical Biol. Med.* **2011**, *51*, 876; g) E. Suarez-Moreira, J. Yun, C. S. Birch, J. H. H. Williams, A. McCaddon, N. E. Brasch, *J. Am. Chem. Soc.* **2009**, *131*, 15078.
- [3] a) L. Ignarro, *J. Cardiovasc. Pharmacol.* **1999**, *34*, 879; b) J. Heinecke, P. C. Ford, *Coord. Chem. Rev.* **2010**, *254*, 235; c) A. A. Avery, *Environ. Health Perspect.* **1999**, *107*, 583.

- [4] W. Carmen, *Med. Hypotheses* **2006**, *67*, 124.
- [5] a) M. J. Rand, C. G. Li, *Eur. J. Pharmacol.* **1993**, *241*, 249; b) S. S. Greenberg, J. Xie, J. M. Zatarain, D. R. Kapusta, M. J. Miller, *J. Pharmacol. Exp. Ther.* **1995**, *273*, 257; c) R. Schubert, U. Krien, I. Wulfesen, D. Schiemann, G. Lehmann, N. Ulfig, R. W. Veh, J. R. Schwarz, H. Gago, *Hypertension* **2004**, *43*, 891.
- [6] F. Jiang, C. G. Li, M. J. Rand, *Eur. J. Pharmacol.* **1997**, *340*, 181.
- [7] M. Brouwer, W. Chamulitrat, G. Ferruzzi, D. L. Sauls, J. B. Weinberg, *Blood* **1996**, *88*, 1857.
- [8] M. Weil, R. Abeles, A. Nachmany, V. Gold, E. Michael, *Cell Death Differ.* **2004**, *11*, 361.
- [9] a) A. Nicolaou, T. Ast, C. V. Garcia, M. M. Anderson, J. M. Gibbons, W. A. Gibbons, *Biochem. Soc. Trans.* **1994**, *22*, 296S; b) A. Nicolaou, S. H. Kenyon, J. M. Gibbons, T. Ast, W. A. Gibbons, *Eur. J. Clin. Invest.* **1996**, *26*, 167; c) A. Nicolaou, C. J. Waterfield, S. H. Kenyon, W. A. Gibbons, *Eur. J. Biochem.* **1997**, *244*, 876; d) A. Kambo, V. S. Sharma, D. E. Casteel, V. L. Woods Jr., R. B. Pilz, G. R. Boss, *J. Biol. Chem.* **2005**, *280*, 10073; e) I. O. Danishpajoo, T. Gudi, Y. Chen, V. G. Khari-tonov, V. S. Sharma, G. R. Boss, *J. Biol. Chem.* **2001**, *276*, 27296.
- [10] a) D. Zheng, R. L. Birke, *J. Am. Chem. Soc.* **2002**, *124*, 9066; b) F. Roncaroli, T. E. Shubina, T. Clark, R. van Eldik, *Inorg. Chem.* **2006**, *45*, 7869; c) M. Wolak, G. Stochel, M. Hamza, R. van Eldik, *Inorg. Chem.* **2000**, *39*, 2018.
- [11] a) M. Wolak, A. Zahl, T. Schnepfenseper, G. Stochel, R. van Eldik, *J. Am. Chem. Soc.* **2001**, *123*, 9780; b) D. Zheng, R. L. Birke, *J. Am. Chem. Soc.* **2001**, *123*, 4637.
- [12] a) T. A. Stich, M. Yamanishi, R. Banerjee, T. C. Brunold, *J. Am. Chem. Soc.* **2005**, *127*, 7660; b) L. Hannibal, J. Kim, N. E. Brasch, S. Wang, D. S. Rosenblatt, R. Banerjee, D. W. Jacobsen, *Mol. Genet. Metab.* **2009**, *97*, 260; c) K. Yamada, R. A. Gravel, T. Toraya, R. G. Matthews, *Proc. Natl. Acad. Sci. USA* **2006**, *103*, 9476; d) F. Watanabe, H. Saido, R. Yamaji, K. Miyatake, Y. Isegawa, A. Ito, T. Yubisui, D. S. Rosenblatt, Y. Nakano, *J. Nutr.* **1996**, *126*, 2947.
- [13] L. Hannibal, C. A. Smith, D. W. Jacobsen, N. E. Brasch, *Angew. Chem.* **2007**, *119*, 5232; *Angew. Chem. Int. Ed.* **2007**, *46*, 5140.
- [14] R. Zhao, J. Lind, G. Merenyi, T. E. Eriksen, *J. Chem. Soc. Perkin Trans. 2* **1997**, 569.
- [15] E. Suarez-Moreira, L. Hannibal, C. A. Smith, R. A. Chavez, D. W. Jacobsen, N. E. Brasch, *Dalton Trans.* **2006**, 5269.
- [16] M. Meier, R. van Eldik, *Inorg. Chem.* **1993**, *32*, 2635.
- [17] L. Xia, A. G. Cregan, L. A. Berben, N. E. Brasch, *Inorg. Chem.* **2004**, *43*, 6848.
- [18] a) A. G. Cregan, N. E. Brasch, R. van Eldik, *Inorg. Chem.* **2001**, *40*, 1430; b) Rate constants k_3 , k_{-3} , k_4 , and k_{-4} from Equation (11) in ref.^[18a] become k_1 , k_{-1} [NO₂], k_2 , and k_{-2} , respectively, in Equation (1) in this article.
- [19] H. M. Marques, L. Knapton, *J. Chem. Soc., Dalton Trans.* **1997**, 3827.
- [20] L. Knapton, H. M. Marques, *Dalton Trans.* **2005**, 889.
- [21] a) J. Wuerges, G. Garau, S. Geremia, S. N. Fedosov, T. E. Petersen, L. Randaccio, *Proc. Natl. Acad. Sci. USA* **2006**, *103*, 4386; b) F. S. Mathews, M. M. Gordon, Z. Chen, K. R. Rajashankar, S. E. Ealick, D. H. Alpers, N. Sukumar, *Proc. Natl. Acad. Sci. USA* **2007**, *104*, 17311.
- [22] D. A. B. Baldwin, E. A. Betterton, J. M. Pratt, *S. Afr. J. Chem.* **1982**, *35*, 173.

Received: February 21, 2013
Published Online: April 29, 2013